PHYSICAL REVIEW B **77**, 081402(R) (2008)

# Charge transport and inhomogeneity near the minimum conductivity point in graphene

Sungjae Cho and Michael S. Fuhrer*

*Department of Physics and Center for Superconductivity Research, University of Maryland, College Park, Maryland 20742, USA*

(Received 28 September 2007; revised manuscript received 5 December 2007; published 11 February 2008)

The magnetic-field-dependent longitudinal and Hall components of the resistivity $\rho_{xx}(H)$ and $\rho_{xy}(H)$ are measured in graphene on silicon dioxide substrates at temperatures $1.6\ \mathrm{K} \leq T \leq 300\ \mathrm{K}$. At charge densities near the minimum conductivity point $\rho_{xx}(H)$ is strongly enhanced and $\rho_{xy}(H)$ is suppressed, indicating nearly equal electron and hole contributions to the current. The data are inconsistent with the standard two-fluid model but consistent with the prediction for inhomogeneously distributed electron and hole regions of equal mobility. At low $T$ and high $H$, $\rho_{xx}(H)$ saturates to a value $\sim h/e^2$, with Hall conductivity $\ll e^2/h$, which may indicate a regime of localized $\upsilon=2$ and $\upsilon=-2$ quantum Hall puddles.

DOI: 10.1103/PhysRevB.77.081402 PACS number(s): 73.63.−b, 73.43.Qt, 81.05.Uw

One of the most fascinating aspects of graphene is that the quasiparticle Hamiltonian is identical to that of massless Dirac fermions, exhibiting a "Dirac point" at which the density of states vanishes linearly without the presence of an energy gap. A striking aspect of experiments is that a finite conductivity is observed in graphene for all charge densities,[1] with a minimum conductivity $\sigma_{xx,min}$ on order $4e^2/h$ (but sometimes significantly smaller[2] or larger,[3,4]), occurring at the minimum conductivity point (MCP); in the absence of disorder, the MCP and Dirac point are identical, but in the presence of disorder, they are slightly different.[4,5] The observation of a finite minimum conductivity has sparked significant theoretical interest. Models invoking only short-range scattering[6,7] give $\sigma_{xx,min}=4e^2/\pi h$ only exactly at the MCP, and fail to reproduce the linear gate-voltage dependence of the conductivity $\sigma_{xx}(V_g)$. Other attempts[8] using the Landauer formalism also obtain $\sigma_{xx} \sim 4e^2/\pi h$ which depends weakly on aspect ratio, but such models are only expected to be valid in the ballistic limit for wide samples, $l < L < W$, where $l$ is the mean free path, $L$ the sample length, $W$ the sample width. Some experiments have probed this limit,[2] but many do not.

Here we show that the conductivity near the MCP is dominated by charge disorder.[5,7,9] In contrast to the *zero* magnetoresistivity expected for pristine graphene, distinct electron and hole puddles[9] give rise to a large magnetoresistivity with functional form consistent with theoretical work on effective media[10] and with a charge density in agreement with a self-consistent theory for Coulomb scattering in graphene.[5] At low temperatures and high magnetic fields the longitudinal resistivity $\rho_{xx}(B)$ saturates to a value $\sim h/e^2$, with Hall conductivity $\sigma_{xy}(B) \ll e^2/h$. The spatially inhomogeneous nature of the MCP[9] indicates that this "plateau"[11–13] may in fact be due to localized $\upsilon=2$ and $\upsilon=-2$ quantum Hall (QHE) puddles.

Our graphene devices are obtained by mechanical exfoliation of Kish graphite on 300 nm $SiO_2/Si$ substrates.[14,15] Figure 1(a) shows an optical micrograph of a completed device; all the data in this paper are from this device. We first characterize the carrier density dependence of the conductivity of this device at zero and high magnetic field. Figure 1(b) shows the longitudinal conductivity $\sigma_{xx}$ as a function of gate voltage $V_g$. The MCP occurs at $V_{g,MCP}=1.7$ V. Away from the MCP, the conductivity increases linearly. The field effect mobility $\mu_{FE}=(1/c_g)d\sigma_{xx}/dV_g$ is 1.6 $m^2/V\,s$ and 2.0 $m^2/V\,s$ for electrons and holes, respectively, where $c_g=1.15\times10^{-4}\ F/m^2$, as determined from the Hall effect at high density.

Figure 1(c) shows $\sigma_{xx}$ and the Hall conductivity $\sigma_{xy}$ as a function of gate voltage at a magnetic field of 8 T.[15,16] The Hall conductivity shows the half-integer quantized plateaux that are a signature of graphene:[1,17] $\sigma_{xy}=\upsilon e^2/h$, with $\upsilon=4(n+1/2)$, $n$ an integer, $e$ the electronic charge, and $h$ the

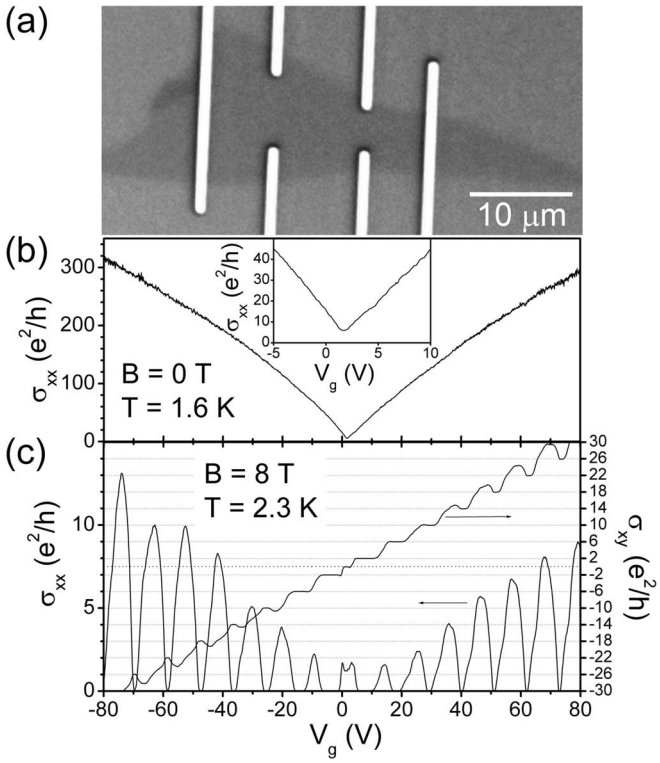


FIG. 1. (a) Optical micrograph of graphene device. Contrast is enhanced to show graphene more clearly. White vertical lines are Cr/Au electrodes, graphene is visible as a slightly darker region compared to the background $SiO_2/Si$ substrate. (b) Longitudinal conductivity $\sigma_{xx}$ as a function of gate voltage $V_g$ at zero magnetic field and temperature of 1.6 K. (c) $\sigma_{xx}$ and Hall conductivity $\sigma_{xy}$ as a function of $V_g$ at magnetic field of 8 T and temperature of 2.3 K.

 

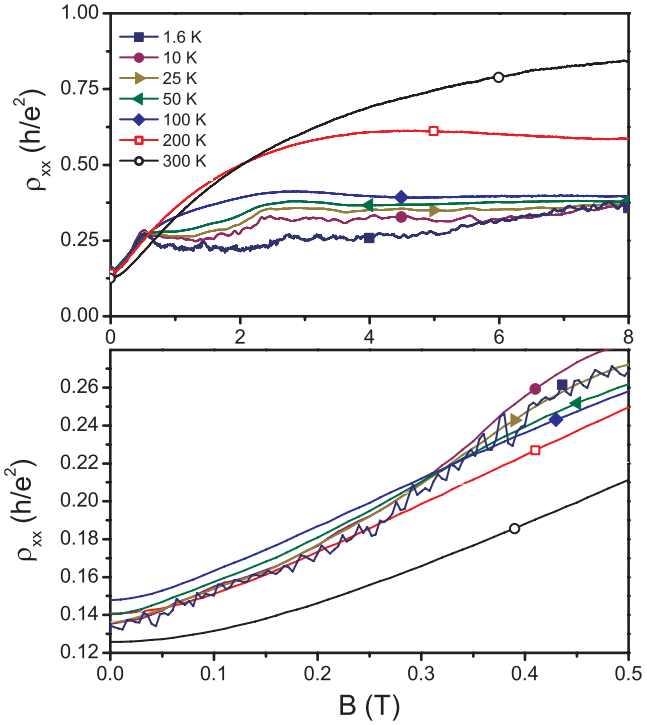


FIG. 2. (Color) Longitudinal resistivity $\rho_{xx}$ as a function of magnetic field $B$ at various temperatures, and a gate voltage of 1.7 V (the point of maximum longitudinal resistivity at zero field). Data are taken on warming from low temperature.

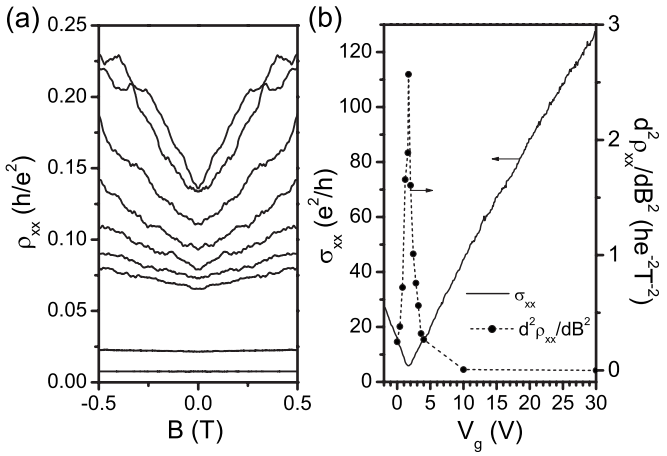


FIG. 3. (a) Longitudinal resistivity $\rho_{xx}$ as a function of magnetic field $B$ at various gate voltages. From top to bottom, curves correspond to gate voltages of 1.7, 2.0, 2.4, 2.8, 3.2, 3.6, 4.0, 10, and 30 V. (b) Longitudinal conductivity $\sigma_{xx}$ (black line, left axis) and the second derivative of the longitudinal resistivity vs magnetic field $d^2\rho_{xx}/dB^2$ at small $B$ (filled circles, right axis) as a function of gate voltage $V_g$ at a temperature of 1.6 K. Dotted line extrapolates between filled circles.

Planck's constant. The plateaulike region $\sigma_{xy} \approx 0$ is also evident.[11–13]

We now discuss the magnetoresistivity $\rho_{xx}(B)$ near the MCP. Figure 2 shows $\rho_{xx}(B)$ at $V_g = 1.7$ V and temperatures from 1.6 K to room temperature. At low fields the magnetoresistivity is roughly temperature independent. At higher fields the resistivity tends to saturate at a value $\sim 0.4h/e^2$ at low temperatures, and increases with no saturation for $B < 8$ T at room temperature. Figure 3 shows the gate voltage dependence of the low-field magnetoresistivity, characterized by the curvature $d^2\rho_{xx}(B)/dB^2$ obtained by fitting $\rho_{xx}(B)$ to a quadratic over the range $-0.2\ \text{T} < B < 0.2$ T. The magnetoresistivity has a sharp peak at the MCP, and falls to near zero at gate voltages more than a few volts from the MCP (at $V_g = 10$ V, the curvature is already 300× lower than at the MCP).

We discuss the possible origins of the positive magnetoresistivity. Weak antilocalization is possible in graphene,[18] and results in a positive magnetoresistivity. However, this effect should saturate at a small magnetic field scale roughly set by the coherence length squared, and should be strongly temperature dependent. Also, consistent with an earlier report,[19] we observe no weak localization or antilocalization at larger gate voltages. Hence we conclude that the magnetoresistivity does not result from weak (anti)localization.

Within the Drude model, a two-dimensional conductor with a single carrier type (e.g., pristine graphene at zero temperature) exhibits no transverse magnetoresistivity, because the force exerted by the Hall field cancels the Lorentz force, and the drift current and resistive voltage are in the same direction. However, a conductor with electrons and holes may exhibit large transverse magnetoresistivity, because the electrons and holes develop components of drift velocity perpendicular to the current which cancel to give zero net transverse current. Both holes and electrons are present at zero temperature in semimetallic graphite, and at finite temperature in graphene. Such a two-fluid model has indeed been proposed to explain the gate voltage dependence of the Hall conductivity in few-layer[20] and single-layer[21] graphene. For a conductor with electrons and holes of concentrations $n$ and $p$ and of equal mobility $\mu$, $\sigma_{xx}^{n,p}(B) = \frac{\sigma_{xx}^{n,p}(0)}{1+(\mu B)^2}$ and $\sigma_{xy}^{n,p}(B) = \pm \frac{\sigma_{xx}^{n,p}(0)\mu B}{1+(\mu B)^2}$, where the positive sign is for electrons, negative for holes, and $\sigma_{xx}^{n,p}(0) = (n,p)e\mu$. Then the resistivity components are

$$\rho_{xx}(B) = \rho_{xx}(0)\frac{1+(\mu B)^2}{1+(\alpha\mu B)^2}, \quad \rho_{xy}(B) = \alpha\rho B\rho_{xx}(B), \quad (1)$$

where $\alpha = (p-n)/(p+n)$. At the MCP, $\alpha = 0$, $\rho_{xx}(B) \propto 1+(\mu B)^2$, and $\rho_{xy} = 0$. Far from the MCP, we expect that $|\alpha| \to 1$ and $\rho_{xx}(B) \approx \rho_{xx}(0)$. This model thus explains *qualitatively* the sharp peak in $\rho_{xx}(B)$ at the MCP (see Fig. 3). However, it does not explain the functional form of $\rho_{xx}(B)$; Fig. 4 shows $\rho_{xx}(B)$ at $T = 300$ K, open circles are the experimental data, while the dotted and dashed-dotted lines are fits to Eq. (1) with $\mu = 1.9\ \text{m}^2/\text{V s}$ and $\alpha = 0$, and $\mu = 2.3\ \text{m}^2/\text{V s}$ and $\alpha = 0.4$ [$\rho_{xx}(0) = 0.125$ in both cases]. In each case $\mu$ is chosen to match the low-$B$ curvature of the resistivity $d^2\rho_{xx}(B)/dB^2 = 2\mu/(1-\alpha^2)$ as determined by a fit to the experimental data for $-0.2\ \text{T} < B < 0.2$ T [Fig. 4(b)]. The fits are poor outside the low-$B$ region. The two-fluid model fails quantitatively in other respects: The near absence of temperature dependence of $\rho_{xx}$ is not explained; at the

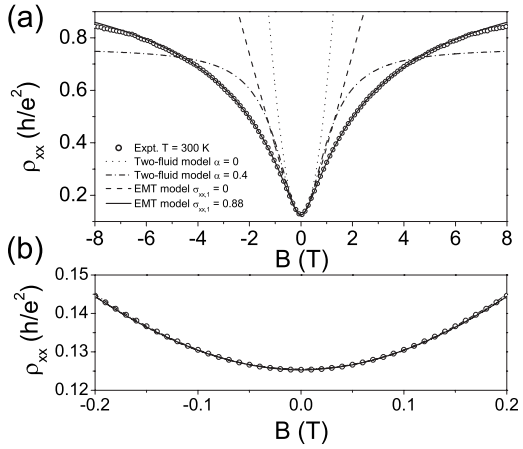


FIG. 4. Longitudinal resistivity $\rho_{xx}$ as a function of magnetic field $B$ at a temperature of 300 K. (a) Open circles are experimental data, dotted line is a fit to the two-fluid model [Eq. (1) in text] with $\alpha=0$, dashed-dotted line is a fit to the two-fluid model with $\alpha=0.4$. The dashed line is a fit to the inhomogeneous model [Eq. (2) in text], and the solid line is a fit to the inhomogeneous model with an additional parallel conductivity [Eq. (3) in text], with $\sigma_{xx,1}=0.88e^2/h$. In all fits, the zero-field resistivity $\rho_{xx}(0)$ and the low-field curvature $d^2\rho_{xx}(B)/dB^2$ are the same, determined by fits to the experimental data at $-0.2\ \mathrm{T}<B<0.2\ \mathrm{T}$, as shown in (b).

MCP, $n=p\approx 0.52(kT/\hbar v_F)^2$, so we expect $\sigma_{xx}(0)=(n+p)e\mu$ to depend quadratically on temperature. At $T=1.6$ K, $n=p\approx 2.3\times 10^6\ \mathrm{cm}^{-2}$, and the peak in $V_g$ should have a width less than 1 mV, not ~2 V as observed in Fig. 3. As discussed previously, another mechanism is already needed to explain the finite conductivity on order $e^2/h$ at the MCP. We put a further constraint on this mechanism: it must also explain the magnetoresistivity at the MCP.

The finite conductivity and the large magnetoresistivity at the MCP together do suggest $p+n$ remains finite while $p-n\rightarrow 0$. There is another scenario in which this is possible: Adam *et al.*[5] propose that local potential fluctuations may induce electron and hole "puddles" in a nominally neutral graphene sheet. Individual graphene samples are characterized by a single parameter, the density of Coulomb impurities $n_{imp}$, which accurately predicts the minimum conductivity, the carrier density at which the MCP appears, and the field-effect mobility. (An additional parameter, the distance of impurities from the graphene sheet, is determined to be 1 nm from the global fit to data from several research groups.) Within this model, the impurity density is given by $n_{imp}=(5\times 10^{15}\ \mathrm{V}^{-1}\ \mathrm{s}^{-1})\mu^{-1}\approx 2.8\times 10^{15}\ \mathrm{m}^{-2}$ for our sample (using $\mu=1.8\ \mathrm{m}^2/\mathrm{V\ s}$, the average field-effect mobility for electrons and holes). At the MCP, the current is carried by an effective carrier density $n^*\approx 1.1\times 10^{15}\ \mathrm{m}^{-2}$, the minimum conductivity is given by $\sigma_{xx,min}=(20e^2/h)(n^*/n_{imp})\approx 7.8e^2/h$, the MCP occurs at a gate voltage $V_{g,MCP}\approx \bar{n}e/c_g=(n_{imp}^2/4n^*)e/c_g=2.5$ V, while the spatial charge inhomogeneity is expected to be important in a region of width $\Delta V_g=2n^*e/c_g=3.0$ V around the MCP. These values are in good agreement with the experimental values $\sigma_{xx,min}=5.9e^2/h$ and $V_{g,MCP}=1.7$ V. $\Delta V_g$ agrees well with both the width of the peak in magnetoresistivity vs $V_g$ in Fig. 3, and the width of the plateau where $\sigma_{xy}\approx 0$ in Fig. 1(b) (~2.1 V). The effective carrier density $n^*\approx 1.1\times 10^{15}\ \mathrm{m}^{-2}$ is larger than the thermally excited carrier density at room temperature $0.8\times 10^{15}\ \mathrm{m}^{-2}$ (see above), so we expect temperature dependence to be small at least up to around room temperature, as observed.

We now discuss the expected magnetoresistivity for the model of Adam *et al.*[5] While the general problem of magnetoresistivity in a spatially inhomogeneous conductor is complex,[22] the magnetoresistivity of an inhomogeneous distribution of electrons and holes with equal mobility and equal concentrations has been solved exactly,[10] and has a simple analytical form,

$$\sigma_{xx}(B)=\sigma_{xx}(0)[1+(\mu B)^2]^{-1/2},\quad \sigma_{xy}(B)=0. \tag{2}$$

Equation (2) predicts a magnetoresistivity which is linear in $B$ at high fields, as shown by the dashed line in Fig. 4, with $\sigma_{xx}(0)=8.0e^2/h$ and $\mu=2.9\ \mathrm{m}^2/\mathrm{V\ s}$. The low-field behavior is consistent with Eq. (2). We find, however, that the fit is greatly improved if Eq. (2) is modified,

$$\rho_{xx}(B)=\left(\sigma_{xx,1}+\frac{\sigma_{xx,0}}{[1+(\mu B)^2]^{1/2}}\right)^{-1}. \tag{3}$$

In Fig. 4, we plot the experimental data (open circles) and a fit to Eq. (3) (solid line) with $\sigma_{xx,0}=7.1e^2/h$, $\sigma_{xx,1}=0.88e^2/h$, and $\mu=3.1\ \mathrm{m}^2/\mathrm{V\ s}$. The fit is excellent. Again, $\rho_{xx}(0)$ and $d^2\rho_{xx}(B)/dB^2=\mu/(1+\sigma_{xx,1}/\sigma_{xx,0})$ are determined by the low-$B$ data alone, leaving only one additional degree of freedom to fit the high-$B$ data. We do not yet understand the origin of the extra conductivity term in Eq. (3), however, it is reasonable to expect deviation from Eq. (2) for several reasons: the electron and hole concentration are not perfectly balanced, the electron and hole mobilities are not equal,[4] and the sample geometry is far from the ideal Hall bar (some current must flow through the electrodes). However, $\sigma_{xx,0}$ is an order of magnitude larger than $\sigma_{xx,1}$, indicating that the bulk of the magnetoresistivity is described by the unusual $[1+(\mu B)^2]^{1/2}$ dependence. From the conductivity and mobility obtained from the fit to Eq. (2) we can obtain a carrier density $n^*_{exp}=\sigma_{xx}(0)/\mu e=6.6\times 10^{14}\ \mathrm{m}^{-2}$. This density is about half the predicted $n^*\approx 1.1\times 10^{15}\ \mathrm{m}^{-2}$. Overall the data suggest that the mobility near the minimum conductivity point is greater than the field-effect mobility; this is consistent with the experimental observation[4] and theoretical prediction of a residual conductivity at the Dirac point.[23]

At low temperatures and high magnetic fields, $\rho_{xx}(B)$ saturates to a constant value $\sim 0.4h/e^2$. Additionally, a plateaulike region of $\sigma_{xy}\approx 0$ is evident in $\sigma_{xy}(V_g)$. This latter feature has been interpreted as an integer quantum Hall effect (QHE) state arising either from the splitting of the valley degeneracy in the $n=0$ Landau level (LL),[12] or due to spin splitting of the 0th LL[11,13] resulting in counterpropagating spin polarized edge states.[13] The latter model gives rise to a dissipative QHE state, in which $\sigma_{xy}$ is only approximately quantized, and $\sigma_{xx}$ is finite. Such a dissipative QHE state would also be expected in spatially inhomogeneous graphene, in which the 0th LL lies below or above the Fermi level in electron or hole regions, respectively. The bulk then

would consist of incompressible electron and hole QHE liquids, separated by regions in which the $n=0$ LL crosses the Fermi level, i.e., fourfold degenerate edge states with counterpropagating modes. From $\mu=2.9\ \mathrm{m}^2/\mathrm{V\,s}$ and $n^*_{\mathrm{exp}}=6.6\times10^{14}\ \mathrm{cm}^{-2}$, we estimate the scattering time $\tau=87$ fs, and the LL broadening $\Lambda\approx\hbar/\tau=7.6$ meV. For $B=8$ T the spacing between the 0th and 1st LL is $\sim100$ meV, the Zeeman energy is $g_{\mu B}=0.9$ meV assuming $g=2$. The average density $n^*_{\mathrm{exp}}$ gives a LL filling factor $\nu=2$ at $B=1.4$ T, and 0.34 at $B=8$ T. Of course, the maximum density within the puddle must be greater than the average density $n^*$, and the QHE occurs over a broad range around the quantized filling factor (for example, the $\nu=+2$ plateau occurs from $\nu=1.1-3.3$), so it is plausible that the puddles could be in the $\nu=\pm2$ QHE states. Recently the imaging of electron and hole puddles in graphene was reported,[24] and the puddle diameter estimated to be $\sim30$ nm. We then expect that quantum effects should be important when the magnetic length is less than the puddle diameter, i.e., $B>0.8$ T, and the temperature is less than $E_F(n^*)$, i.e., $T<350$ K. This is in qualitative agreement with Fig. 2 where significant deviation of $\rho_{xx}(B)$ from Eq. (3) occurs at temperatures $T\leq100$ K and $B\geq0.8$ T, but since Ref. 10 is inadequate to predict the behavior in the quantum regime, more work is needed to understand the high-field low-temperature behavior near the MCP.

This work has been supported by the U.S. ONR Grant No. N000140610882, NSF Grant No. CCF-06-34321, and the UMD-MRSEC (NSF Grant No. DMR-05-20471). We are grateful to S. Adam and S. Das Sarma for useful conversations.

*Author to whom correspondence should be addressed; mfuhrer@umd.edu

[1] K. S. Novoselov, A. K. Geim, S. V. Morozov, D. Jiang, M. I. Katsnelson, I. V. Grigorieva, S. V. Dubonos, and A. A. Firsov, Nature (London) **438**, 197 (2005).

[2] F. Miao, S. Wijeratne, Y. Zhang, U. C. Coskun, W. Bao, and C. N. Lau, Science **317**, 1530 (2007).

[3] J. H. Chen, M. Ishigami, C. Jang, D. R. Hines, M. S. Fuhrer, and E. D. Williams Adv. Mater. (Weinheim, Ger.) **19**, 3623 (2007).

[4] J. H. Chen, C. Jang, M. S. Fuhrer, E. D. Williams, and M. Ishigami, arXiv:0708.2408 (unpublished).

[5] S. Adam, E. H. Hwang, V. M. Galitski, and S. D. Sarma, Proc. Natl. Acad. Sci. U.S.A. **104**, 18392 (2007).

[6] T. Ando, J. Phys. Soc. Jpn. **75**, 074716 (2006); K. Ziegler, Phys. Rev. Lett. **97**, 266802 (2006).

[7] K. Nomura and A. H. MacDonald, Phys. Rev. Lett. **98**, 076602 (2007).

[8] M. I. Katsnelson, Eur. Phys. J. B **51**, 157 (2006); J. Tworzydlo, B. Trauzettel, M. Titov, A. Rycerz, and C. W. J. Beenakker, Phys. Rev. Lett. **96**, 246802 (2006).

[9] E. H. Hwang, S. Adam, and S. Das Sarma, Phys. Rev. Lett. **98**, 186806 (2007).

[10] V. Guttal and D. Stroud, Phys. Rev. B **71**, 201304(R) (2005).

[11] Z. Jiang, Y. Zhang, H. L. Stormer, and P. Kim, Phys. Rev. Lett. **99**, 106802 (2007).

[12] Y. Zhang, Z. Jiang, J. P. Small, M. S. Purewal, Y. W. Tan, M. Fazlollahi, J. D. Chudow, J. A. Jasczak, H. L. Stormer, and P. Kim, Phys. Rev. Lett. **96**, 136806 (2006).

[13] D. A. Abanin, K. S. Novoselov, U. Zeitler, P. A. Lee, A. K. Geim, and L. S. Levitov, Phys. Rev. Lett. **98**, 196806 (2007).

[14] K. S. Novoselov, D. Jiang, F. Schedin, T. J. Booth, V.V. Khotkevich, S. V. Morozov, and A. K. Geim, Proc. Natl. Acad. Sci. U.S.A. **102**, 10451 (2005).

[15] See EPAPS Document No. E-PRBMDO-77-R01808 for discussion of sample preparation and determination of sample resistivity from resistance. For more information on EPAPS, see http://www.aip.org/pubservs/epaps.html.

[16] Because the sample is not an ideal Hall bar, we estimate a maximun error of 19% in determining the numerical factor of proportionality between the longitudinal resistivity and the resistance.[15] However, error in this numerical factor will only rescale the vertical axes of Figs. 1(b), 2(a), 2(b), and 3 (left and right), and 4. Figure 1(c) would be modified, however the half-integer QHE plateaus are unchanged since $\rho_{xx}$ is zero there, and we find that the $\nu=0$ plateau is insensitive to changing the numerical factor by as much as a factor of 2. Crosstalk between the longitudinal and Hall measurements is eliminated by taking the symmetric and antisymmetric components of the magnetic field dependences, respectively (subtracted components are always $<10\%$ of the total).

[17] Y. Zhang, Y.-W. Tan, H. L. Stormer, and P. Kim, Nature (London) **438**, 201 (2005).

[18] T.Ando and T. Nakanishi, J. Phys. Soc. Jpn. **67**, 1704 (1998); X. Wu, X. Li, Z. Song, C. Berger, and W. A. de Heer, Phys. Rev. Lett. **98**, 136801 (2007); E. McCann, K. Kechedzhi, V. I. Falko, H. Suzuura, T. Ando, and B. L. Altshuler, *ibid.* **97**, 146805 (2006).

[19] S. V. Morozov, K. S. Novoselov, M. I. Katsnelson, F. Schedin, L. A. Ponomarenko, D. Jiang, and A. K. Geim, Phys. Rev. Lett. **97**, 016801 (2006).

[20] K. S. Novoselov, A. K. Geim, S. V. Morozov, D. Jiang, Y. Zhang, S. V. Dubonos, I. V. Grigorieva, and A. A. Firsov, Science **306**, 666 (2004).

[21] E. H. Hwang, S. Adam, and S. Das Sarma, Phys. Rev. B **76**, 195421 (2007).

[22] R. Magier and D. J. Bergman, Phys. Rev. B **74**, 094423 (2006).

[23] M. Trushin and J. Schliemann, Phys. Rev. Lett. **99**, 216602 (2007); X.-Z. Yan, Y. Romiah, and C. S. Ting, arXiv:0708.1569 (unpublished).

[24] J. Martin, N. Akerman, G. Ulbricht, T. Lohmann, J. H. Smet, K. von Klitzing, and A. Yacoby, Nat. Phys. **4**, 148 (2008).